ARL

US Army Research Laboratory

US Army Research Laboratory (ARL) Standard for Characterization of Electric-Field Sensors, 10 Hz to 10 kHz

by Sean M Heintzelman

NOTICES

Disclaimers

The findings in this report are not to be construed as an official Department of the Army position unless so designated by other authorized documents.

Citation of manufacturer's or trade names does not constitute an official endorsement or approval of the use thereof.

Destroy this report when it is no longer needed. Do not return it to the originator.

US Army Research Laboratory

US Army Research Laboratory (ARL) Standard for Characterization of Electric-Field Sensors, 10 Hz to 10 kHz

by Sean M Heintzelman
Sensors Electron and Devices Directorate, ARL

REPORT DOCUMENTATION PAGE			*Form Approved* *OMB No. 0704-0188*

Public reporting burden for this collection of information is estimated to average 1 hour per response, including the time for reviewing instructions, searching existing data sources, gathering and maintaining the data needed, and completing and reviewing the collection information. Send comments regarding this burden estimate or any other aspect of this collection of information, including suggestions for reducing the burden, to Department of Defense, Washington Headquarters Services, Directorate for Information Operations and Reports (0704-0188), 1215 Jefferson Davis Highway, Suite 1204, Arlington, VA 22202-4302. Respondents should be aware that notwithstanding any other provision of law, no person shall be subject to any penalty for failing to comply with a collection of information if it does not display a currently valid OMB control number.
PLEASE DO NOT RETURN YOUR FORM TO THE ABOVE ADDRESS.

1. REPORT DATE *(DD-MM-YYYY)* November 2016	2. REPORT TYPE Technical Report		3. DATES COVERED (From - To) 03/2012–09/2016
4. TITLE AND SUBTITLE US Army Research Laboratory (ARL) Standard for Characterization of Electric-Field Sensors, 10 Hz to 10 kHz			5a. CONTRACT NUMBER
			5b. GRANT NUMBER
			5c. PROGRAM ELEMENT NUMBER
6. AUTHOR(S) Sean M Heintzelman			5d. PROJECT NUMBER
			5e. TASK NUMBER
			5f. WORK UNIT NUMBER
7. PERFORMING ORGANIZATION NAME(S) AND ADDRESS(ES) US Army Research Laboratory ATTN: RDRL-SES-P 2800 Powder Mill Road Adelphi, MD 20783-1138			8. PERFORMING ORGANIZATION REPORT NUMBER ARL-TR-7880
9. SPONSORING/MONITORING AGENCY NAME(S) AND ADDRESS(ES)			10. SPONSOR/MONITOR'S ACRONYM(S)
			11. SPONSOR/MONITOR'S REPORT NUMBER(S)

12. DISTRIBUTION/AVAILABILITY STATEMENT
Approved for public release; distribution unlimited.

13. SUPPLEMENTARY NOTES

14. ABSTRACT

The US Army Research Laboratory (ARL) has designed and build a one-of-a-kind electric-field sensor characterization facility. The unique facility features a large parallel plate capacitor with guard rings to control fringing fields, controlled by a custom LabVIEW program and several pieces of test hardware with less than 0.6% combined measurement error. ARL's electric-field characterization facility creates an approximately 1-m^3 region with better than 1.5% electric-field uniformity in a smaller physical system than that described in the Institute of Electrical and Electronics Engineers Standard 1308-1994. The custom-developed LabVIEW code thoroughly tests the frequency response, linearity, total harmonic distortion, and noise across a 60-dB frequency range of an electric-field sensor in less than 10 min. The instrumentation, calibration, and characterization methods are detailed.

15. SUBJECT TERMS
electric field, sensors, characterization, LabVIEW, sensor testing

16. SECURITY CLASSIFICATION OF:			17. LIMITATION OF ABSTRACT	18. NUMBER OF PAGES	19a. NAME OF RESPONSIBLE PERSON Sean M Heintzelman
a. REPORT Unclassified	b. ABSTRACT Unclassified	c. THIS PAGE Unclassified	UU	52	19b. TELEPHONE NUMBER (Include area code) 301-394-3151

Standard Form 298 (Rev. 8/98)
Prescribed by ANSI Std. Z39.18

Contents

List of Figures

INTENTIONALLY LEFT BLANK.

1. Introduction

Electric-field sensors use a conductor of known size and conductivity to collect charge on their transducers, followed by analog circuitry and signal processing to output a voltage proportional to the electric field at the sensor interface.

Electric-field sensors generally fall into 3 categories. Electric-field mills use a shutter to repeatedly expose and shield a conductor to measure it in a charged and uncharged state, respectively, and are suited to static and subkilohertz fields.[1] A second sensor approach is to measure ΔV between 2 conductors at a fixed separation d, in a configuration the US Army Research Laboratory (ARL) has named a "potential gradiometer".[2] A third method of sensing quasi-static fields is to use ground reference sensors (GRSs), where 2 conductors are connected through a transimpedance amplifier to measure dE/dt as a function of dq/dt on the source conductor relative to the sink conductor.[3] Sensors using the second and third methods have been characterized at ARL, with results documented in Appendix A of this report.

The electric field $\boldsymbol{E}$ created by an point charge with arbitrary magnitude $Q(t)$ in free space is given from Coulomb's law:

$$\boldsymbol{E}(t) = \frac{Q(t)}{4\pi\varepsilon_0}\frac{\hat{r}}{|\vec{r}|^2} \ , \tag{1}$$

where $\boldsymbol{r}$ is a vector representing the field coordinates relative to the source charge and ε_0 is the permittivity of free space. If instead the electric potential V is known for 2 sides of a parallel plate capacitor, then the electric-field magnitude can easily be approximated as

$$E(t) = \frac{\Delta V(t)}{d} \ , \tag{2}$$

where ΔV is the potential difference between the 2 plates and d is the distance between them. Equations 1 and 2 provide the basis of electric-field sensing in the "near zone" of electric-field sources, meaning they can be used to calculate both static and quasi-static electric fields.

The Institute of Electrical and Electronics Engineers (IEEE) Standard (Std) 1308-1994[4] provides a method for generating uniform electric fields that allow testing of electric-field sensors, shown on the Fig. 1. A voltage generator connected to a center-tapped transformer is used to differentially drive 2 parallel square conductors (called "endplates"), separated up to half the distance of the side length. The configuration also requires that any conductor placed in the geometric center

of the plates is small, so the uniformity of the field remains within 1%. The sensor should not exceed 0.23 m in its largest diagonal direction for a 1.5×1.5 m endplate configuration,[5] with no ground planes within 0.5 m of the endplates.
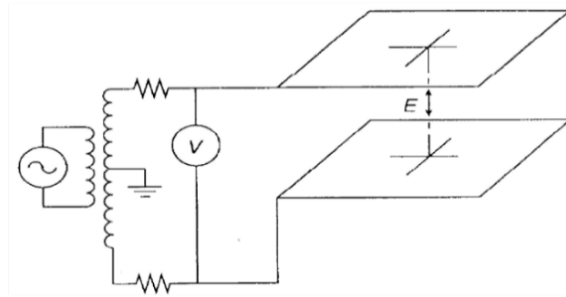
Fig. 1   IEEE Std 1308-1994[4] recommended configuration for calibrating electric-field sensors

At ARL, we have interest in characterizing sensors up to 1 m in the largest diagonal direction, meaning IEEE Std 1308-2006[4] suggests the endplates must be about 6.5×6.5-m with 3.25-m separation. With the additional 0.5-m separation from ground planes or a Faraday cage, one needs a $7.5 \times 7.5 \times 4.5$ m laboratory just to hold the testing system. Conversely, if we take a more reasonable laboratory size of 3×3 m, the IEEE standard restricts the system to $2 \times 2 \times 1$ m size and therefore the sensor size to 0.31 m in the largest diagonal direction. This complication presents a need to design an electric-field sensor characterization facility with a larger uniform area in a smaller system size.

To overcome these problems, a conductive shield is used with a linear potential gradient along its length from the endplate potentials +V to –V (Fig. 2). This reduces capacitance between the endplates and external conductors while also lowering capacitance between the shield and the endplates, both of which mitigate noise in sensor measurements. The ARL electric-field cage (Fig. 2) was designed on this principle by using "guard tubes" connected by resistors to reinforce a linear potential along the length of the electric-field cage.[6]
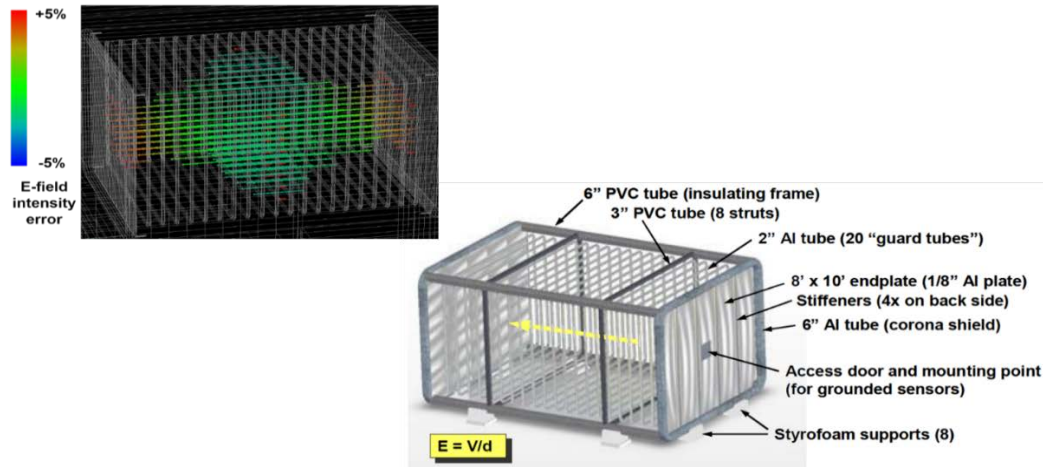
Fig. 2 **(Left) ARL electric-field cage model showing the percent error in electric-field accuracy at all points within 5% of the electric-field magnitude and within 0.5° of the field direction. (Right) Computer-aided design model of the ARL electric-field cage with insulated mounting.**

Modeling using ARL method of moments (MoM) software shows the center of the cage provides an approximately 1-m^3 volume (greater than 1.2-m largest diagonal distance), where a known electric field is generated with less than 1.5% error.[6] To verify the performance of our cage with sensor-like objects inside, we use ARL MoM software to show the distortion in electric-field intensity of various-sized conducting spheres. This distortion is compared to the distortion of the spheres in a uniform electric field, the IEEE-standard calibration system, and the QUASAR Federal System's calibration system based of the IEEE standard.[7] The results of the 3 cages relative to the free space model are shown in Fig. 3.
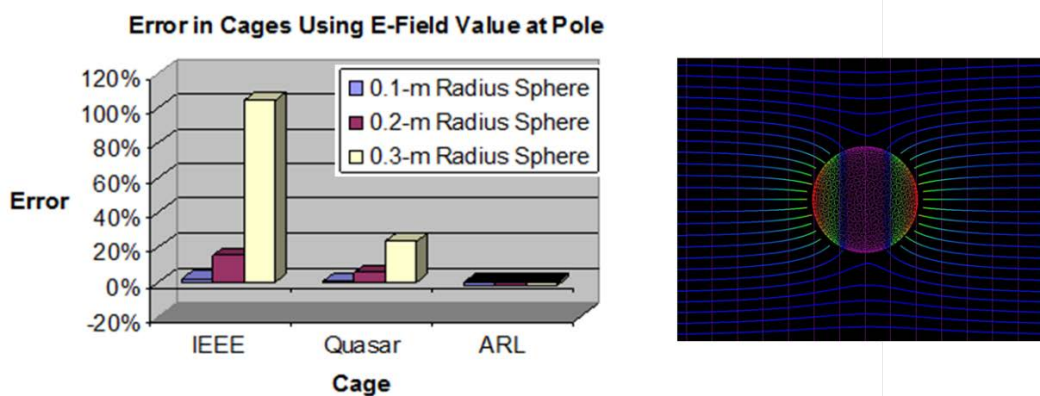
Fig. 3 **(Left) The error in electric-field intensity of conducting spheres placed at the center of different electric-field cage designs. The field intensity is evaluated at the 2 outer points of the sphere closest to the endplates, and the error is derived by comparison to the sphere modeled in free space (right).**

3

All 3 sensing modalities can be characterized easily in the ARL electric-field cage due to an access door on one of the endplates (GRS modality) and a nonconductive mount in the center (potential gradiometer and field mill modalities). Four unique testing configurations with the ARL electric-field cage are pictured in Fig. 4.
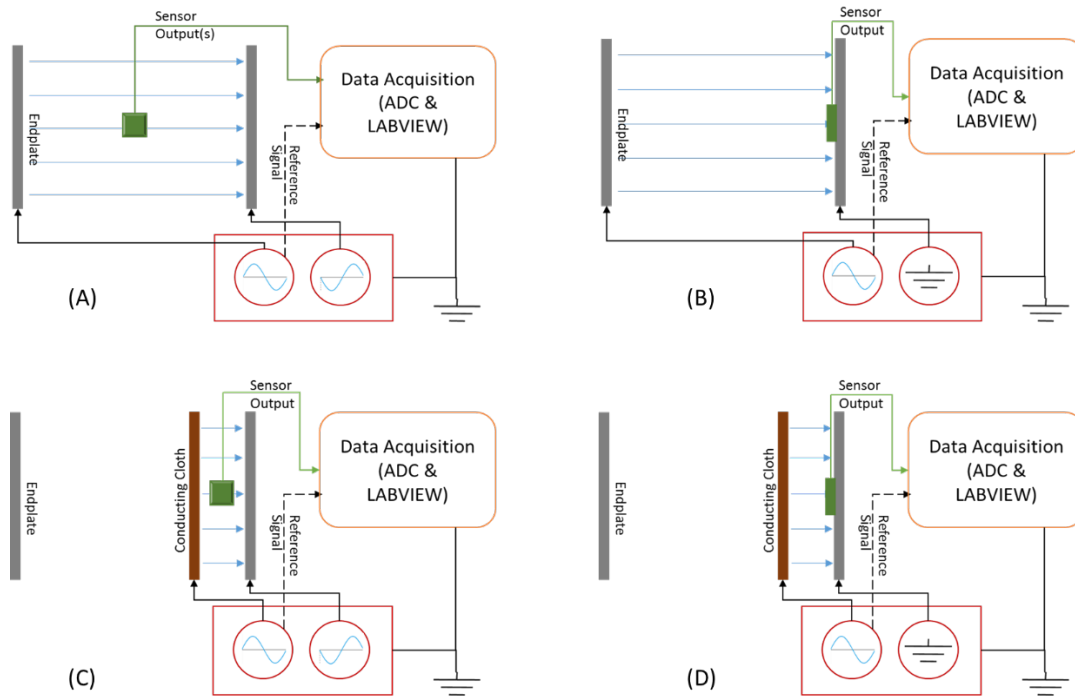
Fig. 4 **Four ARL electric-field cage hardware configurations for sensor calibration with no guard tubes drawn. (A) Electrically floating sensor in a bipolar field. (B) Large GRS in a unipolar field. (C) Testing small electrically floating sensors in a high-strength bipolar field. A conducting fabric is connected to the guard tube and creates a temporary endplate within the IEEE-recommended s/2 spacing. (D) Testing small GRS in a higher-strength unipolar field.**

Figure 4 shows the high-level hardware and software components used in electric-field sensor characterization, including structural modification to test within IEEE Std 1308 guidelines. Additionally, ARL is interested in automating characterization (calibration) routines for our sensors to reduce test times and human error. Various hardware was purchased and LabVIEW software was custom-developed to create a rigorous and autonomous characterization system.

2. Hardware Used for Autonomous Operation

2.1 Data Acquisition Chassis

Data acquisition and basic signal processing during a characterization test is handled by a Peripheral Component Interconnect Extensions for Instrumentation

(PXIe) 1062Q is an 8-channel LabVIEW express chassis. The rear panel provides connectors (Ethernet, Bayonet Neill–Concelman [BNC], etc.) that can be used for communication with external hardware devices (i.e., function generators). One PXI card used with the PXIe 1062Q in our experiment is the PXIe8101 with an Intel 2-GHz embedded controller. The LabVIEW software code runs on this Intel processor, and the controller PXI card provides connections for communication/ data transfer.

2.2 Analog-to-Digital Converter (ADC)

To measure the reference signal (dotted black line) in Fig. 4a–d and up to 3 analog sensor outputs during characterization tests, a PXI4462 4-channel 24-bit analog-to-digital converter (ADC) is used. An NI9239 4-channel ADC is also used in parallel to provide 8 total channels for measurements. Of the sensors presented in Appendix A, none required more than one ADC for characterization. These 2 ADCs can be used interchangeably due to their similarities dynamic range and noise floors, and the sensors have been characterized with both ADCs.

2.3 Arbitrary Waveform (Function) Generator

The waveform generator is used to create necessary electric potential at the ARL electric-field cage endplates. The function generator creates single-ended or differential (180° out of phase) sinusoidal voltages on the 2 output channels, as well as provides an in-phase transistor–transistor logic (TTL) trigger output referenced to the first channel. To reduce time-domain phase shifts from this trigger for our sub-100-kHz frequencies, we use a 2-m BNC cable. We also use an Agilent 33522A function generator.

2.4 Serial/Ethernet Port and Current Preamplifier (Optional Components)

Data need to be transferred between the hardware pieces and the LabVIEW chassis, and each hardware piece can have different serial speeds. The SR 2016 is a 16-port gigabit switch device that allows serial interfacing the chassis and multiple-speed hardware devices, which interfaces the hardware devices to the LabVIEW software. In most of our experiments, it is used to interface between the PXIe 1062Q and the waveform generator only.

A current to voltage amplifier is needed for sensors with true current outputs, such as an SR 570 amplifier. A current preamplifier allows us to add low-pass filtering and variable gain levels to the sensor output to better suit the PXI4462's voltage input requirements. The current amplifier settings should be tracked by the user

since the device is manually controlled (not by LabVIEW code) and these settings are necessary during postexperiment data processing.

Figure 5 shows the physical connections between all hardware components listed in this section. Details of the custom software code developed in LabVIEW are provided in Appendixes B and C.
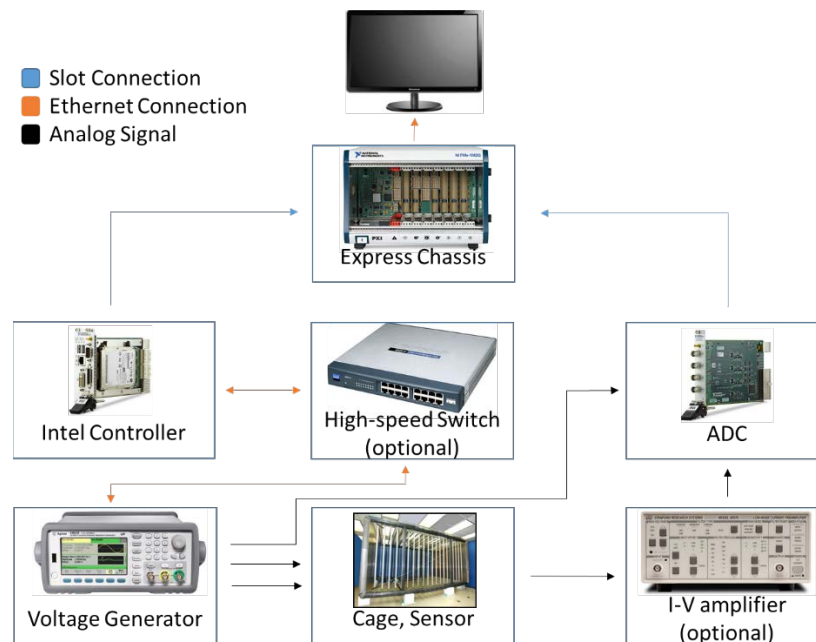
Fig. 5   Setup and wiring for autonomous characterization of sensors with the electric-field cage

3.   Characterizing Capabilities for Electric-field Sensors

This section details the performance of the ARL electric-field cage connected in parallel to the ADC, with the function generator as the source signal. This characterizes the operational accuracy of the electric-field cage excitations used for sensor measurements and serves as a corollary to documented measurements[6] of electric-field accuracy over the cage volume.

3.1 Frequency Response

While electric-field sensors directly measure an electric field, their outputs are read as voltages. Data sheets typically provide a sensitivity value, the voltage output per unit of field over a specific frequency band, for sensors. The frequency response of a sensor describes how sensor output voltage changes in response to electric field as the frequency varies and is an important factor in our voltage to electric-field mapping. Frequency responses are typically measured with phase-locked loops

(PLLs) or fast Fourier transform (FFT) measurements at the appropriate frequency bin, and while ARL can perform both measurements types, ARL predominantly uses the FFT-based method.

For most sensor characterization tests, we use a standard matrix of 5 magnitudes spaced approximately an order of magnitude (20 dB) apart and 31 frequency points spaced equally on a logarithmic scale ($f_{n+1} = 1.259f_n$). The exact values of the matrix are presented as points in Fig. 6.
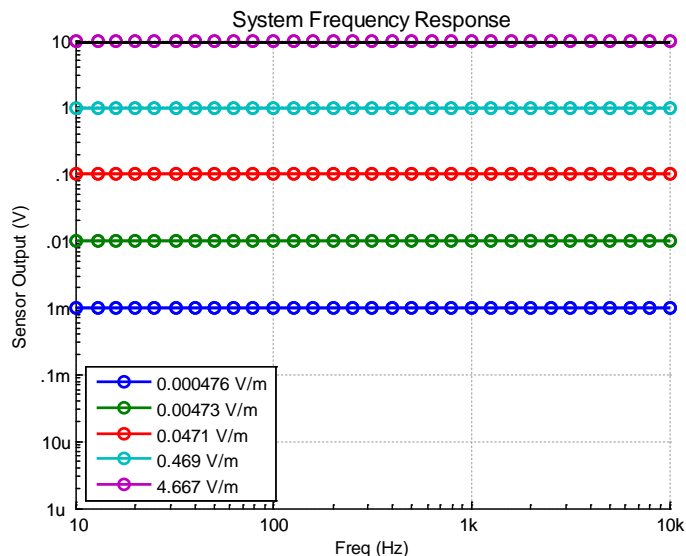
Fig. 6   Frequency response of our 31 × 5 test matrix used for standard sensor characterization

The frequency response allows us to calculate the sensitivity of each sensor at different frequency values. The sensitivity provides an estimate on the maximum electric field the sensor can reliably measure. An ideal sensor will have a single value that can be applied throughout the entire frequency band and rated dynamic range of the sensor, although circuitry and device physics usually cause deviations near the edges of this range.

The sensitivity value, derived from frequency response, can also be used to reliably approximate the upper end of the sensor's dynamic range. The sensor's maximum output voltage can be divided by a sensor's sensitivity value, giving the maximum electric-field magnitude our sensor can reliably measure.

The sensitivity can be considered for the ARL electric-field cage itself. We apply 19.6 V across the endplates to produce a 4.67-V/m field, meaning the sensitivity χ is 4.2 V/(V/m) or 4.2 m; the separation distance of our cage endplates. Real sensors will have a less trivial and nonlinear sensitivity dependence due to effects from transducers, amplifiers, and so on.

The error in the applied electric-field strength also must be characterized for the system, which gives us the maximum error in sensor sensitivity calculations. Results from Fig. 7 are used for sensor characterization within the 0%–0.55% error values reflected in the graph. The values are used to create correction factors at each test point in the frequency response matrix, allowing postmeasurement processing to reduce system errors to under 0.1%.
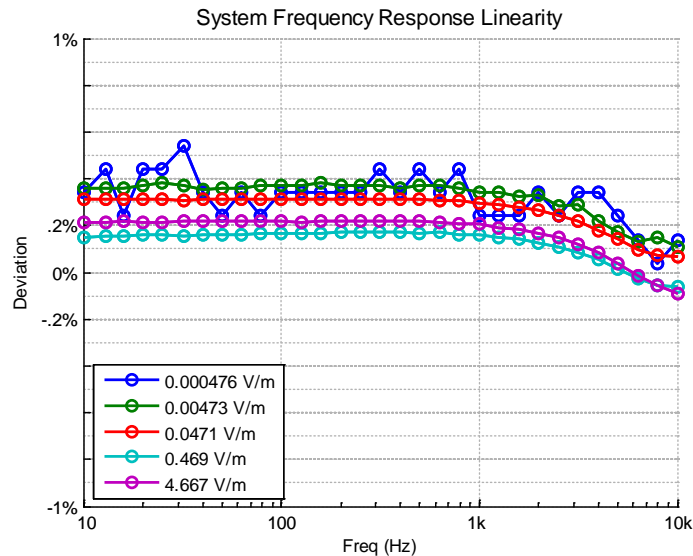
Fig. 7   The ARL characterization system error as a function of frequency. The error remains under 0.6% over an 80-dB bandwidth.

For sensor characterization tests where only 1% accuracy is desired, however, an averaged value from Fig. 7 can be used for the "calibration of measurement system" variable described in Appendix B.

3.2 Phase Response

The phase response measures how much an electric-field sensor output lags behind the electric-field cage endplate excitation potential. The phase response is a function of the sensor transducer, filters, gain circuitry, nonlinearity, and so on. This measurement is simply the phase portion of the FFT taken during the frequency response. For our system phase response, we measure the phase of the second endplate referenced to the endplate in phase with the function generator's TTL signal. The results are presented in Fig. 8.
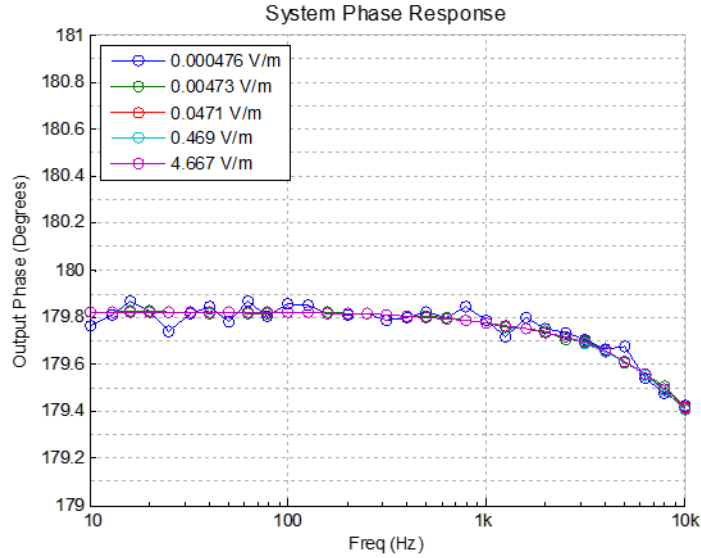
Fig. 8   Phase response of our 31 × 5 test matrix used for standard sensor characterization

As can be seen in Appendix A, our system has a more linear phase response than many commercial off-the-shelf and Government off-the-shelf sensors. The system phase response results show the ARL characterization system is within with 0.6° of ideal linearity up to 10 kHz. The results from Fig. 8, much like the results from Fig. 7, are used to derive correction factors for sub-1% accuracy sensor characterizations.

3.3 Noise Spectral Density

We measure the voltage noise floor or noise spectral density (NSD) of these sensors as a function of frequency to determine the lower limit of the sensor's dynamic range. In laboratory environments, one is often limited by electric-field noise that exists in the measurement equipment and especially at power harmonics. To limit these environmental noise effects, we de-energize all noncritical lab equipment during testing. The resulting system NSD is shown in Fig. 9.
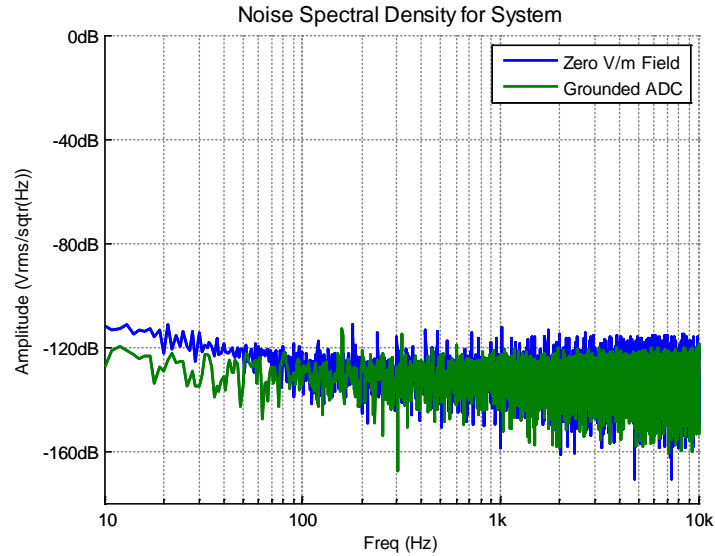
Fig. 9   The voltage NSD of the ARL characterization system, where the endplates are connected in parallel to the ADC to account for cage impedances

The NSD measurement must first be normalized into volts per root hertz, or V/√(Hz), if the FFT bin size is not exactly 1 Hz already. For example, a 10-s FFT measurement requires the 10 FFT bins, which represent the equivalent single-hertz bin width (e.g., 0.5–1.4 Hz bins representing a 1-Hz bin) to be summed together. The NSD is then divided at each frequency bin by the sensor's sensitivity value to determine the electric-field-referred noise spectral density (EFNSD) of the sensor, shown in Fig. 10.
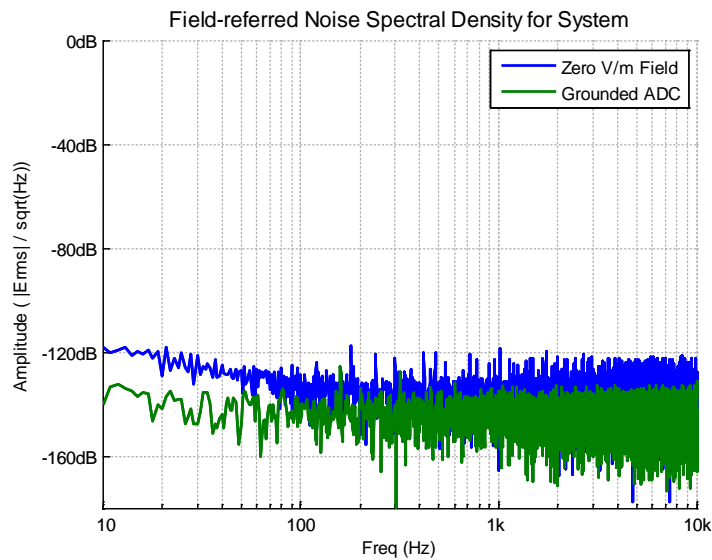
Fig. 10   The EFNSD of the ARL characterization system

10

We have performed an EFNSD measurement on our system as shown in Fig. 10 by dividing each bin in the NSD measurement by the sensitivity value of the system, 4.2. For this report, all EFNSD graphs are reported in electric-field magnitude per root hertz, or $|E|/\sqrt{(Hz)}$, since this is similar to the common $V/\sqrt{(Hz)}$ representation in sensor literature.

With both the maximum and minimal detectable electric-field values being determined from the frequency response and EFNSD graphs, the frequency-dependent dynamic range of a sensor can then be calculated:

$$Dynamic\ Range\ \left(dB\frac{V}{m}\right) = 20 * log\left\{\frac{V_{MO}}{\chi}\right\} - 20 * log\{E_{min}\}\ , \qquad (3)$$

where V_{MO} is the maximum output voltage of the sensor and E_{min} corresponds to a selected frequency value from the EFNSD measurement. This dynamic range value would ideally be constant, but environmental effects and circuit nonlinearity create a frequency dependence of the dynamic range value.

From the frequency response and EFNSD measurements, our system is found to have approximately 140 dB of dynamic range at the 316-Hz midband frequency and at least 130-dB dynamic range throughout the entire testing bandwidth. Therefore, sensors with dynamic ranges over these values are limited by the ARL characterization system.

3.4 Linearity

Sensor linearity for our sensor characterization system refers to ability to maintain a voltage output directly proportional to the electric-field strength when held at a single frequency. An ideal sensor produces a consistent χ value for any selected frequency within its rated bandwidth. The data acquired during the frequency response also provide the data needed to characterize the linearity of the ARL system and are presented in Fig. 11.
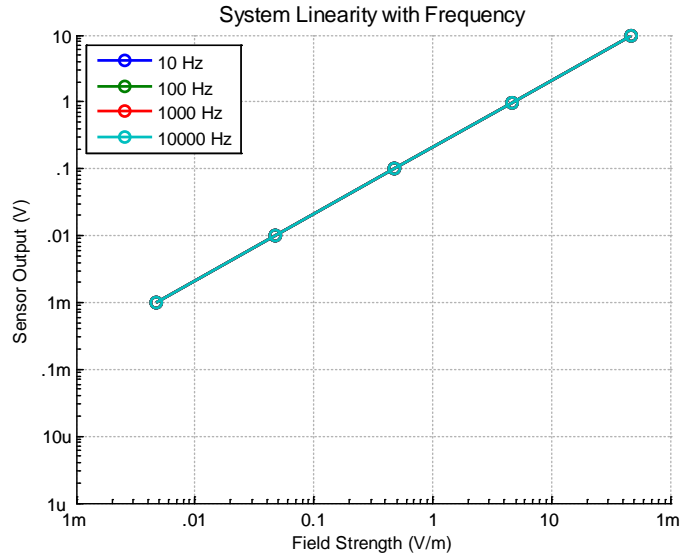
Fig. 11   Linearity of the ARL sensor characterization system over an 80-dB range of field strengths

To calculate percent linearity for our sensor across the measurement bandwidth, we select the sensitivity value at the logarithmic midpoint of the frequency bandwidth (316 Hz at 4.667 V/m) and find its ratio with the sensitivity at other frequencies. The results are shown in Fig. 12.
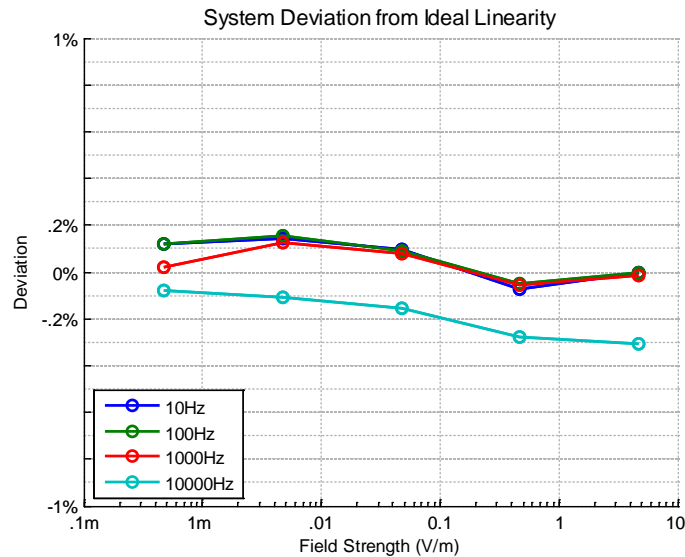
Fig. 12   The ARL characterization system linearity as a function of electric-field strength remains within ±0.3% at each order of magnitude in our 80-dB bandwidth

If a sensor is perfectly linear (i.e., $\chi_{316\ Hz} / \chi_f$ is exactly 1), the deviation from linearity is precisely 0%. This calculation of linearity for this report is defined as

$$SYSTEM\ LINEARITY\ =\ max\left\{\sum_{f=10}^{f=10000}\left|1-\frac{\chi_{316\ Hz}}{\chi_f}\right|*100\%\right\},\qquad(4)$$

where f denotes any of the 31 test frequencies from the frequency response.

3.5 Total Harmonic Distortion (THD)

When in the presence of a monotone sinusoidal electric field, an ideal electric-field sensor output will be a proportional monotone sinusoid. The ratio of energy in the sensed harmonic tones relative to the energy at the fundamental frequency is known as total harmonic distortion (THD), which can be calculated as

$$THD\ =\ \left(\sum_{n=2}^{n=\infty}\frac{V_n}{V_1}\right)*100\%\ ,\qquad(5)$$

where V_1 is the FFT amplitude of the sensor output at the fundamental frequency and V_n is the FFT amplitude at the nth harmonic.

To avoid power harmonics for the first 15 harmonics and complement the NSD bandwidth, a 93-Hz fundamental frequency is selected and measured with a 1-s FFT to calculate the sensor THD. For this report, we truncate the THD calculation at the 20th harmonic since the results show a signal-to-noise ratio value near 1 starting near 2 kHz. The ARL characterization system THD has been measured with the endplates connected in parallel to the ADC, with results shown in Fig. 13.
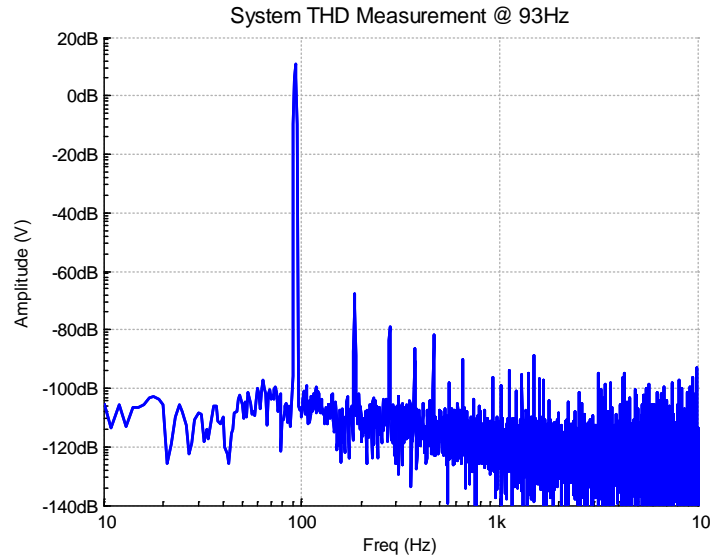
Fig. 13   **The 0.05% THD of the ARL system is shown. The results provide validation that sensor THD can be characterized with better than 0.1% accuracy.**

4. Conclusions and Future Work

This report has presented the theory, design, and performance of the ARL electric-field cage and how it is used to characterize electric-field sensors. Electrical measurements have demonstrated the uncalibrated hardware system to have less than 0.6% error in magnitude and less than 0.6° error in phase, therefore providing a reliable environment for electric-field sensor characterization. Improvements are currently being made to the testing facility to allow greater electric-field strengths to be generated while maintaining 1% linearity over a 100-kHz bandwidth.

5.   References

1. About electric field mill operation. Tuscon (AZ): Mission Instruments; 2006 [accessed 2016]. http://www.missioninstruments.com/pages/learning/about_fm.html.

2. Hull D, Heintzelman S. Characterization and analysis of electric-field sensors. 2015 IEEE. Industry Applications Society Annual Meeting; 2015 Oct 18–22; Dallas, TX. doi: 10.1109/IAS.2015.7356747.

3. Heintzelman S. Self-adjusting quasi-static electric-field sensor. Electrostatic Society of America; 2016 [accessed 2016]. http://www.electrostatics.org/images/O1.pdf.

4. IEEE recommended practice for instrumentation: specifications for magnetic flux density and electric field strength meters - 10 Hz to 3 kHz. Piscataway (NJ): IEEE Power Engineering Society; 1995 (reaffirmed 2001, 2010). Report No.: 1308-1994. doi: 10.1109/IEEESTD.1995.79525.

5. Takuma T, Kawamoto T, Sunaga Y. Analysis of calibration arrangements for AC field strength meters. IEEE Trans Power Apparatus and Systems. 1985; PER-5(2):489–496. doi: 10.1109/TPAS.1985.319065.

6. Hull D. ARL electric-field cage modeling, design, and fabrication. Military Sensing Symposium; 2005 Aug 23–25; Baltimore, MD.

7. QUASAR Federal Systems homepage. San Diego (CA): QUASAR Federal Systems; 2016 [accessed 2016]. http://www.quasarfs.com/.

INTENTIONALLY LEFT BLANK.

Appendix A. Results and Analysis of Various Electric-field Sensors

A-1 Plessey EPIC

Figures A-1 through A-3 show 2 PS25102 sensors[1] spaced 60 mm apart with differential output.
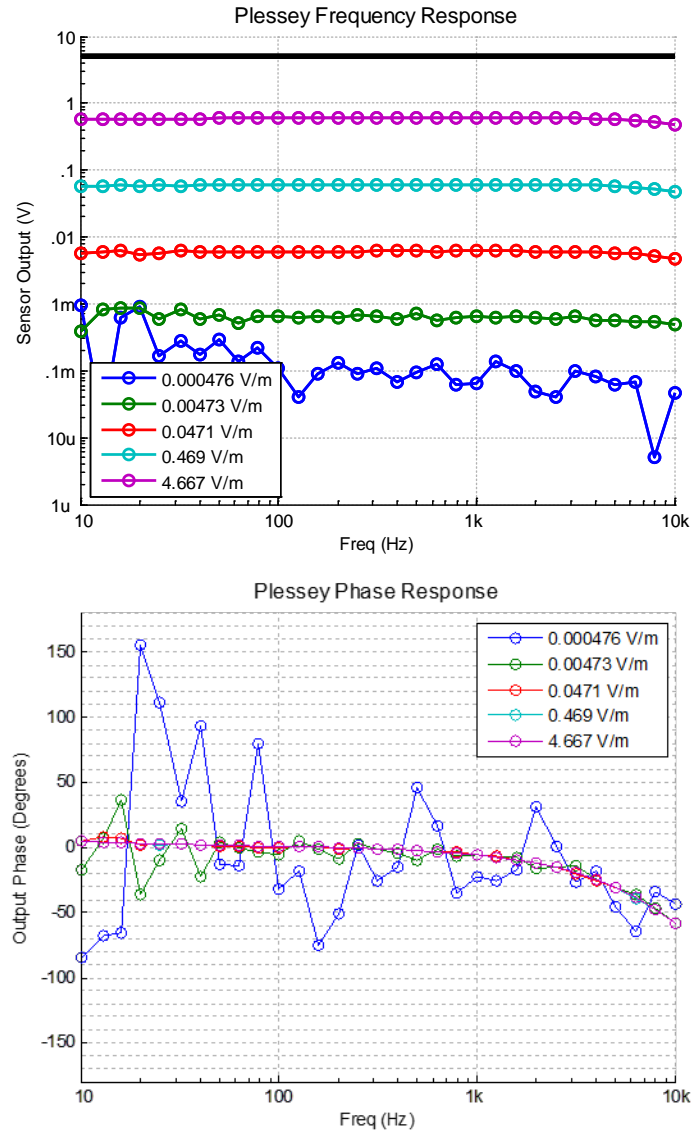
Fig. A-1 PS25102 sensors' frequency and phase responses

[1] Plessey Semiconductors homepage. Devon (UK): Plessey Semiconductors; n.d. [accessed 2016]. http://www.plesseysemiconductors.com/epic-plessey-semiconductors.php.

Fig. A-2 PS25102 sensors' deviation from the 316-Hz sensitivity value and linearity
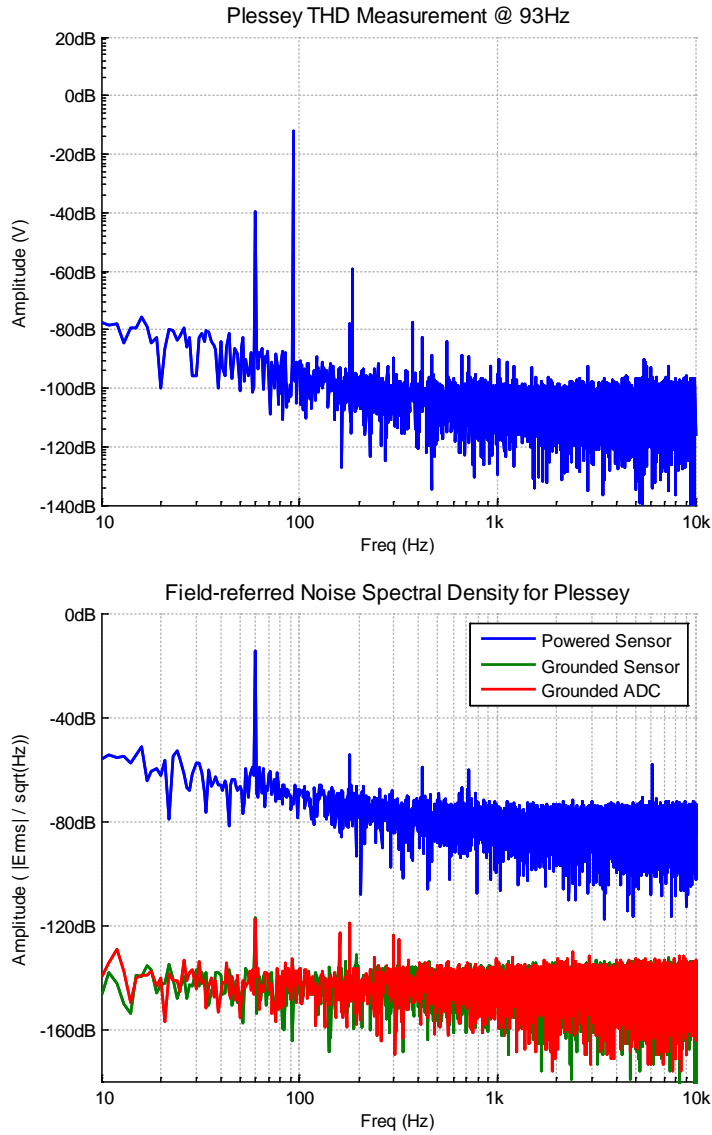
Fig. A-3 PS25102 sensors' measurements for THD and ERNSD

Note: Total harmonic distortion (THD) = 0.8%, dynamic range (316 Hz) = 100 dB, and sensitivity (316 Hz) = 130 mV/(V/m).

A-2 QUASAR RVS

Figures A-4 through A-6 show 2 voltage detection sensors (QUASAR[2]) spaced 60 mm apart with differential output.
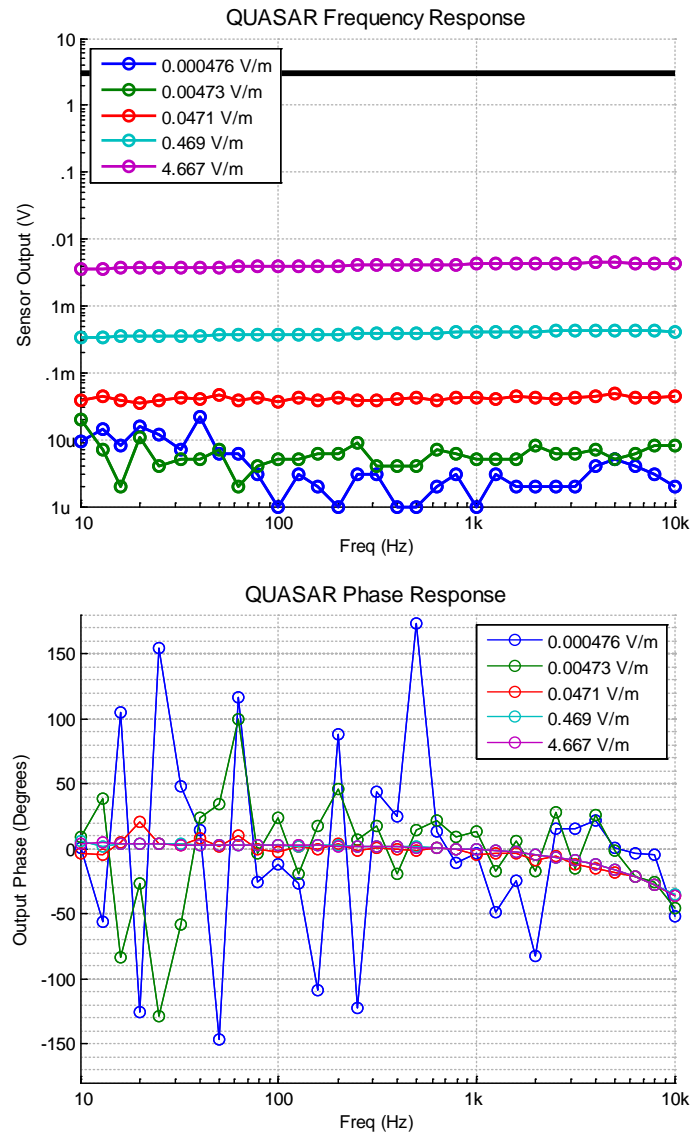
Fig. A-4 QUASAR sensors' frequency and phase responses

[2] QUASAR Federal Systems homepage. San Diego (CA): QUASAR Federal Systems; 2016 [accessed 2016]. http://www.quasarfs.com/.
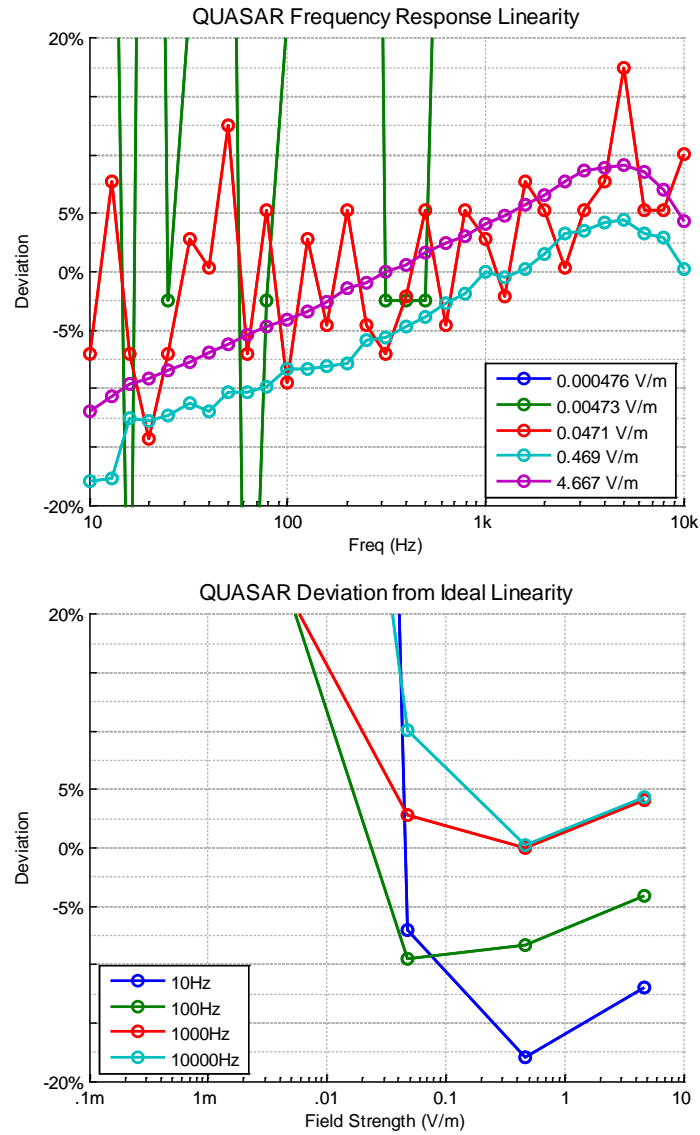
Fig. A-5 QUASAR sensors' deviation from the 316-Hz sensitivity value and linearity
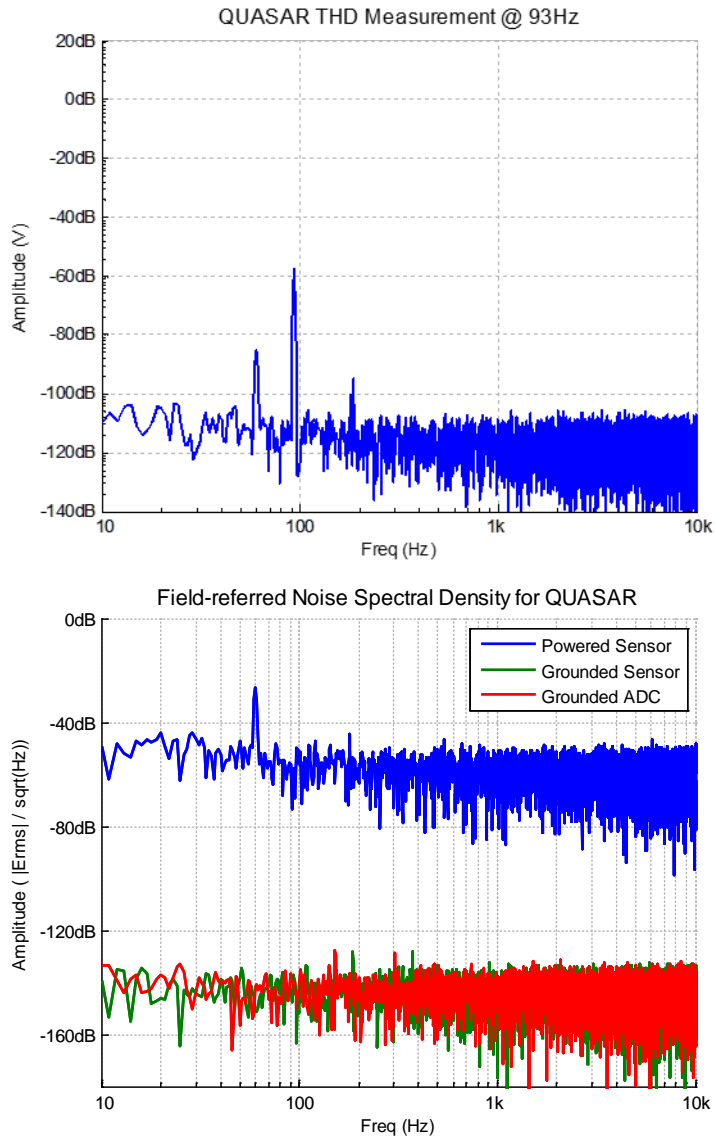
Fig. A-6   QUASAR sensors' measurements for THD and ERNSD

Note: THD = 2.6%, dynamic range (316 Hz) = 110dB, and sensitivity (316 Hz) = 870 μV/(V/m)

A-3 ARL Smart D-dot

Figures A-7 through A-9 show one d-dot sensor[3] tested in the cage configuration pictured in Fig. 4d in the report.
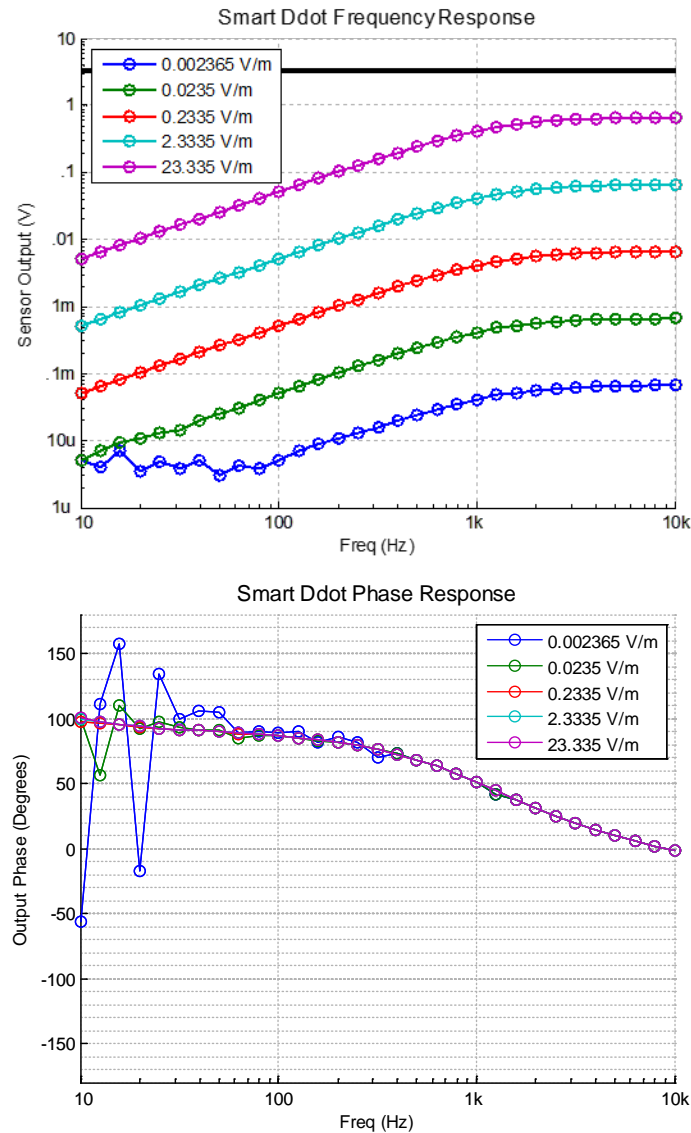
Fig. A-7 D-dot sensor's frequency and phase responses

---

[3] Heintzelman S. Self-adjusting quasi-static electric-field sensor. Electrostatic Society of America; 2016 [accessed 2016]. http://www.electrostatics.org/images/O1.pdf.
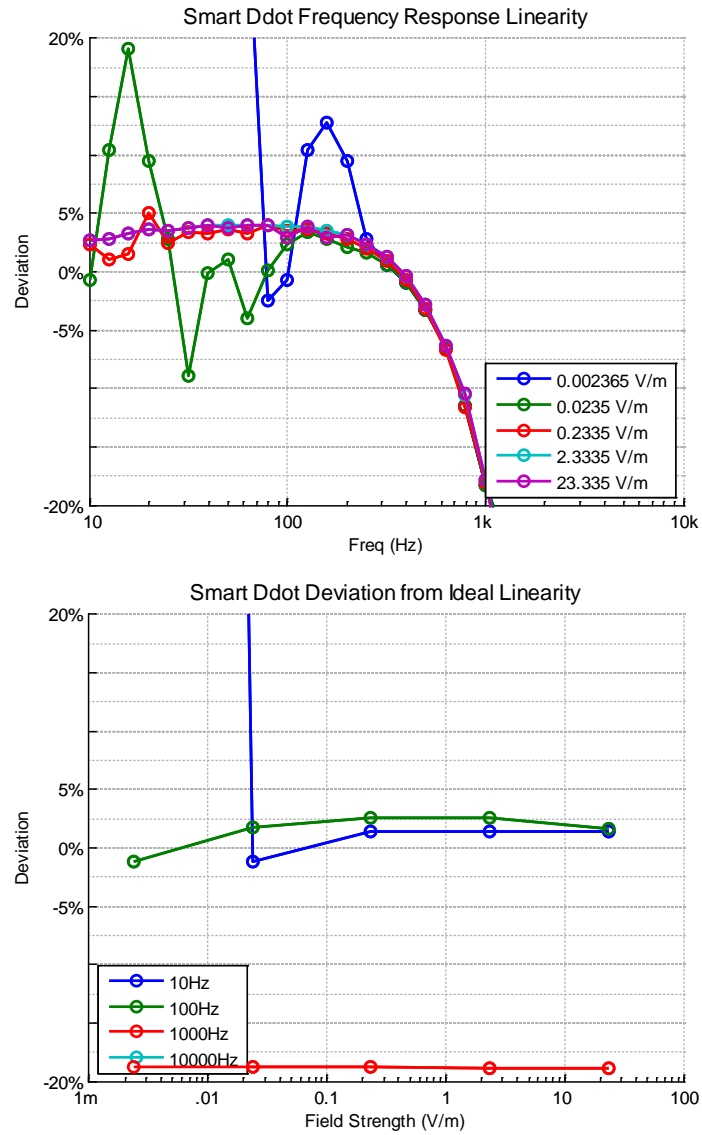
Fig. A-8 D-dot sensor's deviation from the 316-Hz sensitivity value and linearity
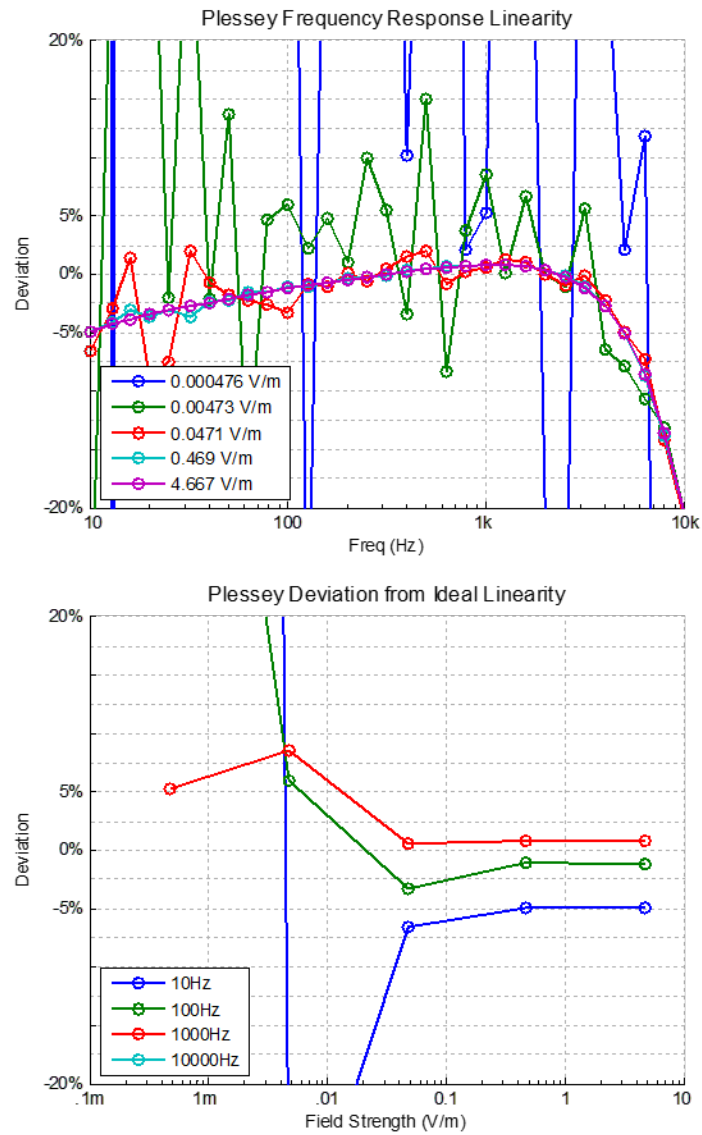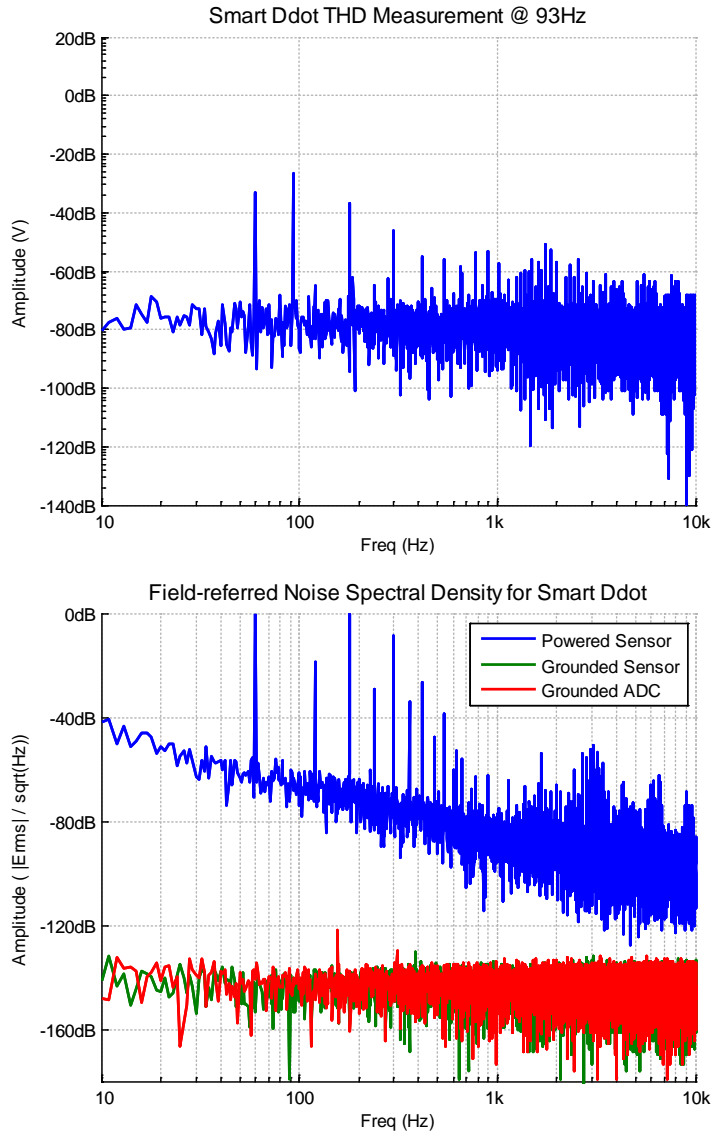
Fig. A-9 D-dot sensor's measurements for THD and ERNSD

Note: THD = 2.8%, dynamic range (316 Hz) = 120dB, and sensitivity (316 Hz) = 6.9 mV/(V/m).

Appendix B. Operation of the Electric-field Cage

B-1 Checklist for testing

1. Mount the desired sensor according to Fig. 4 in the report and connect necessary wires for powering and measuring the device output (battery, Bayonet Neill-Concelman [BNC], Ethernet, etc.).

2. Connect all power outlets on the function generator, Peripheral Component Interconnect Extensions for Instrumentation (PXIe) 1062Q, current preamplifier, and/or Ethernet switch to a battery or isolated power outlet.

3. Use BNC cables to connect the 2 outputs of the Agilent 33522A signal generator to each electric-field cage endplate. Set the output the impedance to 50 ohm.

4. Insert the analog-to-digital converter (ADC) and Intel controller cards into available slots on the PXI1062Q chassis. The choice of slots is up to the user since LabVIEW software should automatically recognize and map the ports/connections on each PXI card to correct names in the main LabVIEW code. Connect the NI9239 ADC to a USB port on the computer, if desired.

5. Use a BNC cable to connect the function generator trigger output to an analog input on the ADC. Any channel can be used for the trigger/reference signal; however, the software program defaults to Ai0 (analog input 0) and should be changed to reflect otherwise.

6. Connect the "active link" port on the PXIe8101 to one of the SR 2016's communication channels with Ethernet cable. Connect a second Ethernet cable between SR 2016 and the local area network port on the Agilent 33522A.

7. Use VGA to USB cable/adaptor between the PXIe8101 port and a computer display.

8. If sensor outputs are current outputs, configure the SR570 to appropriate filter and gain settings. Take manual note of these setting for postprocessing of the characterization data.

9. Connect sensor outputs to available ports on PXI4462 and/or the NI9239 ADC(s).

10. Ensure LabVIEW DAQmx software, appropriate drivers, and needed updates have been downloaded from the National Instruments website (http://www.ni.com/en-us.html).

11. Use LabVIEW "Measurement and Automation Explorer" to confirm proper hardware connections and communication capabilities. All devices should have a green check mark to the left of their name, and settings can be configured appropriately for the device under test.

12. Load the "Efield Testing" LabVIEW project on monitor and load the "SH Standardized Characterization" virtual instrument (VI). The program should load all sub-VIs and the front panel appears when complete.

B-2 Front Panel Navigation

The front panel of SH Simple Data Collection Sweep.vi is shown in Fig. B-1.
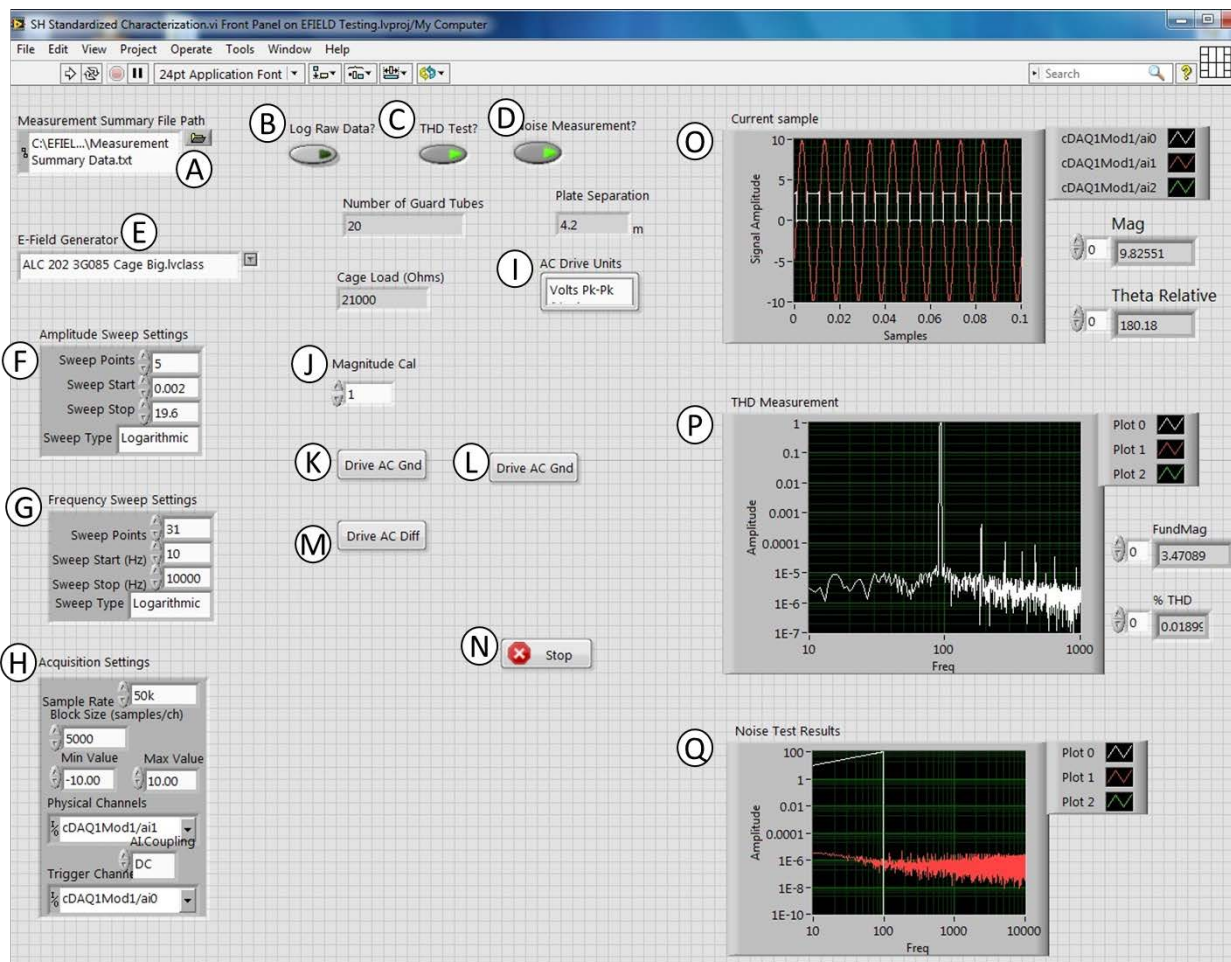

Fig. B-1 Front panel diagram of the autonomous characterization scheme used for sensor characterization at the US Army Research Laboratory

The left side of the front panel contains inputs for the VI, while the right side will display measurements while the program is running. Each component labeled is explained as follows:

(A) *Measurement Summary File Path.* This contains the file hierarchy and file name, which will record the summary data for the measurement. To change the name or path of the file, select the folder icon next to this box. Navigate to the proper folder on the hard drive and create a .txt file if one is not already created. Copy the file path and filename, then paste into the text area of this control on the front panel.

(B) *Log Raw Data?* This Boolean control displays bright green when true and a forest green when false. A "true" setting logs the raw samples collected by the PXI4462 as a .csv file for every trigger channel and physical channel(s) during the entire test duration. The data should match the "Total Measurements" front panel waveform when plotted in Excel or MATLAB.

(C) *THD Test?* This Boolean when selected will run a total harmonic distortion test for the sensor and capture the measurement as a .csv file. A 1- or 10-s sample will be taken to compute the fast Fourier transform (FFT) based on block-diagram settings.

(D) *Noise Measurement?* A "true" setting on this Boolean collects 1 s of continuous samples of all PXI4462 channels at 50 kS/s and performs a software FFT on the data, and the measurement length can be increased in software as desired. The FFT results are saved as a .csv file for simple plotting in MATLAB or Excel, and should match the "Noise Test Results" front panel waveform.

(E) *E-field Generator.* The arrow along the right side of this control is used to select the electric-field cage being used for the measurement. The choice for most tests is "ALC 202 3G085 Cage Big.lvlclass" (Fig. 4a or b configurations) or "ALC 202 3G085 Cage Small.lvlclass" (Fig. 4c or d configurations). When the play button is selected and the test begins to run, the appropriate values for the selected cage configuration with populate the "Number of Guard Tubes", "Plate Separation", and "Cage Load (Ohms)" indicators. The values are logged in one of the posttest data files, and plate separation is used to calculate the electric-field strength for logging in the data files.

(F) *Amplitude Sweep Settings.* This LabVIEW custom datatype has 4 individual controls for the user. "Sweep Points" is an integer for the number of voltage amplitudes to sweep through for the frequency response measurement. "Sweep Start" is a 3-decimal float for the lowest voltage to apply to the electric-field cage endplates. "Sweep Stop" is a 3-decimal float for the highest voltage to apply to the endplates. "Sweep Type" selects linear or

logarithmic spacing between the amplitude points when the "Sweep Points" control is greater than 2.

(G) *Frequency Sweep Settings.* This LabVIEW custom datatype has 4 individual controls for the user. "Sweep Points" is an integer for the number of frequency amplitudes to sweep through for the measurement. "Sweep Start" is a 3-decimal float for the lowest frequency at the electric-field cage endplates. "Sweep Stop" is a 3-decimal float for the highest frequency to the endplates. "Sweep Type" selects linear or logarithmic spacing between the frequency points when "Sweep Points" has a value greater than 2.

(H) *Acquisition Settings.* A custom datatype is used to control the ADCs connected to the LabVIEW chassis. "Sample Rate" refers to the acquisition speed of the ADC, and should be kept at least 2.4 times higher than the maximum test frequency to safely meet Nyquist criteria. "Block Size (samples/ch)" controls the number of captured samples to be used with the optional phase-locked loop (PLL) measurement algorithm. "Min Value" and "Max Value" icons determine the voltage range that will be accepted by the ADC measurements and should be just greater than the "Sweep Stop" value of the "Amplitude Sweep Settings" datatype. "Trigger Channels" and "Physical Channels" select the ports on the PXI4462 to use as the phase reference and signal channels, respectively. "AI Coupling" selects whether to use AC or DC coupling on the ADC analog inputs during characterization.

(I) *AC Drive Units.* This control contains a list of 8 enumerated settings used to correlate the amplitudes in the "Amplitude Sweep Settings" to function generator voltage outputs. The true Agilent 33522A outputs determines the "V" used to calculate the applied electric field (*E=V/d*, d is the "Plate Separation" value) logged in the measurement summary file.

(J) *Magnitude Cal.* This value is a correction factor based on small hardware errors in the testing system. To calculate the appropriate value, see Section B-3.

(K) *Drive AC Gnd.* This button control is used to initiate tests with the ground reference sensors (GRSs). One endplate will have the applied voltage determined by the "Amplitude Sweep Settings" while the other endplate is kept at ground.

(L) *Averaged THD.* This button initiates only the FFT portion of the sensor characterization test, but repeats the FFT measurement 100 times by default to create an averaged THD measurement.

(M) *Drive AC Diff.* This button control is used to initiate tests where a fully differential electric field is desired for the measurement. Each endplate will have the applied voltage determined by the "Amplitude Sweep Settings" and will be 180° out of phase with one another. This maximizes the electric-field strength compared to the single-ended configuration.

(N) *Stop.* This button will cancel the current measurement at any point during the sweep. Can cause issues with saving/opening the generated data files, use only when necessary.

(O) *Current Lockin Sample.* This waveform graph displays the data sample captured by the PXI4462 during the current sweep setting. The time difference between points and total number of points are determined by the sample rate and measured samples per ADC channel. The "mag" and "Theta Relative" numbers to the right of this graph populate with the measured sensor magnitude and phase, respectively.

(P) *THD Measurement.* This waveform graph displays the result of the most recent THD measurement. The "FundMag" and "% THD" blocks reflect the strength of the fundamental tone in volts and the THD value for the first 5 harmonics, respectively.

(Q) *Noise Test Results.* This waveform graph displays the results for current portion of the sensor noise measurement in volts per hertz. MATLAB postprocessing gets the data from this graph into a more readable form.

B-3 Calibration of Measurement System

To normalize any voltage gain/attenuation caused by all characterization system hardware, we perform a basic calibration of the system. The calibration scalar can be determined using the function generator:

1. Connect one output from the function generator to any ADC analog input. This might require disconnecting on of the sensor's outputs temporarily.

2. Set the "Physical Channel" under acquisition settings on the LabVIEW front panel to the channel selected in step 1.

3. Select a single voltage amplitude of 1 V and a single frequency between 10–10000 Hz by modifying the "Amplitude Sweep Settings" and "Frequency Sweep Settings" appropriately.

4. Ensure "Magnitude Cal" on the front panel is set to 1.

5. Press the play then "Drive AC Diff" buttons. The experiment will run for less than 10 s before finishing.

6. The 3-decimal float populating the "R" indicator on the front panel should be populated. Calculating 1/R gives the calibration constant; the scalar multiple difference between the actual input voltage and measured voltage.

7. The calculated calibration constant should be entered in the "Magnitude Cal" block of the front panel. Sensor outputs during characterization will be multiplied by this constant to negate the sensor effects due to this small error in the test hardware.

B-4 Making a Sensor Characterization Measurement

After following the methods of Sections B-1 to B-3, a sensor characterization is ready to be completed:

1. Note the ADC inputs which the Agilent 33522A transistor–transistor logic (TTL) signal and sensor output(s) are connected. These should reflect the values in the "Acquisition Settings" "Trigger Channels" and "Physical Channels" blocks. For correct syntax, use LabVIEW standards.[1]

2. Input the desired sweep settings in the "Amplitude Sweep Settings", "Frequency Sweep Settings", and "AC Drive Units" for the characterization.

3. Select appropriate Boolean values for recording the raw data collected by the ADC, the THD measurement, and/or the noise tests.

4. Press the play button on the front panel diagram. The button should darken in color.

5. Press either the "Drive AC Gnd" or "Drive AC Diff" button to begin the measurement sequence. The play button on the front panel will release or turn lighter in color when the test is complete, or if "Stop" button is pressed during a measurement.

6. View summary files to ensure the data was updated with the newest characterization test results. Copy and rename the .txt summary file as a .csv file to be saved/exported when data processing begins.

---

[1] What is the syntax for physical channel strings in DAQmx? Austin (TX): National Instruments; 2014 [accessed 2016]. http://digital.ni.com/ public.nsf/allkb/9A2AF5E10E0C893386256FE8006807DF.

INTENTIONALLY LEFT BLANK.

Appendix C. LabVIEW Electric-field Cage Control

The flow diagram (Fig. C-1) represents 3 different test sequences corresponding to the 3 different executables that can be selected on the LabVIEW front panel. The "Drive AC Diff" and "Drive AC Gnd" executables follow similar paths, with the only difference being whether one of the endplates is held at ground (unipolar field) or tracking 180° out of phase (bipolar field). This Appendix details how inputs from the LabVIEW front panel are used in the test sequence of the first 2 columns pictured in Fig. C-1, while the "Averaged THD" column will not be described due to its straightforwardness.
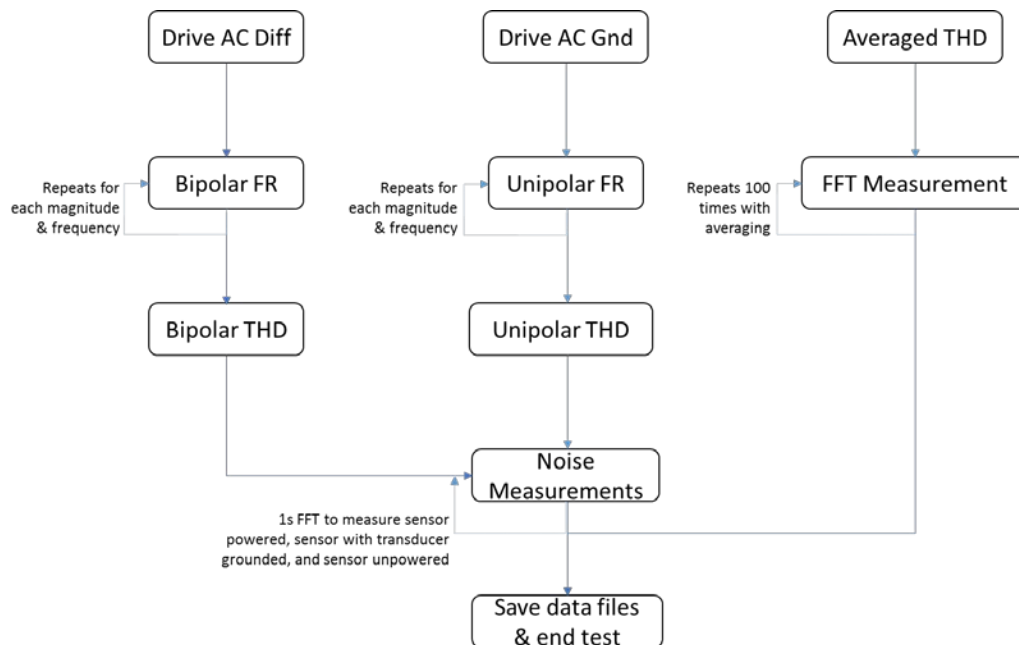
Fig. C-1 The test sequences of 3 executable options

C-1 Configuration

The US Army Research Laboratory (ARL) electric-field cage "object" (Fig. C-2) is loaded (1) with its associated properties: plate separation, number of guard tubes, and cage load in ohms. The communication with the function generator is verified (2). All other front panel inputs are passed into the main graphical user interface loop to determine proper automation sequencing.
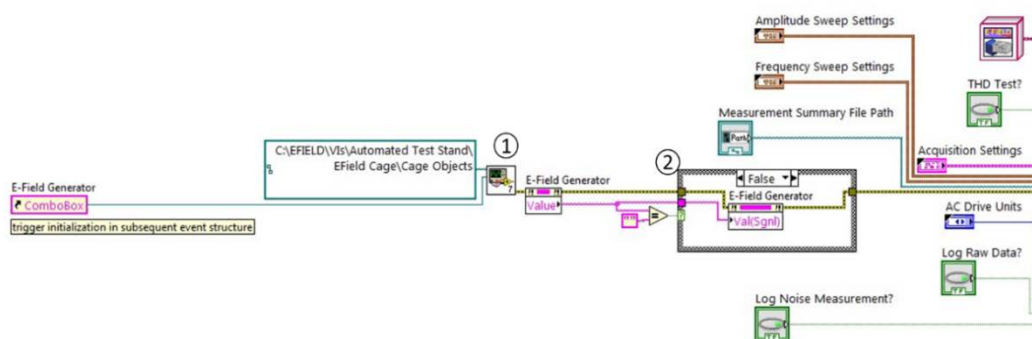
Fig. C-2 Reading and loading input values for the characterization test

C-2 FR, Linearity, and PR Measurement

The frequency sweep settings and amplitude sweep settings (Fig. C-3) are passed into sub-virtual instruments (VIs) (2) and (3), which create 2 arrays of voltage and frequency values of size M and N, respectively, and thereby our M×N test matrix for the frequency response. An Excel spreadsheet is also created (4) with appropriate header labels (5) to track the frequency response. The "plate separation" parameter is extracted (1) from the electric-field cage object, and the acquisition setting parameters are separated (6) for individual use later in the program.

Fig. C-3 Processing input parameters to select and load proper values into the test sequence

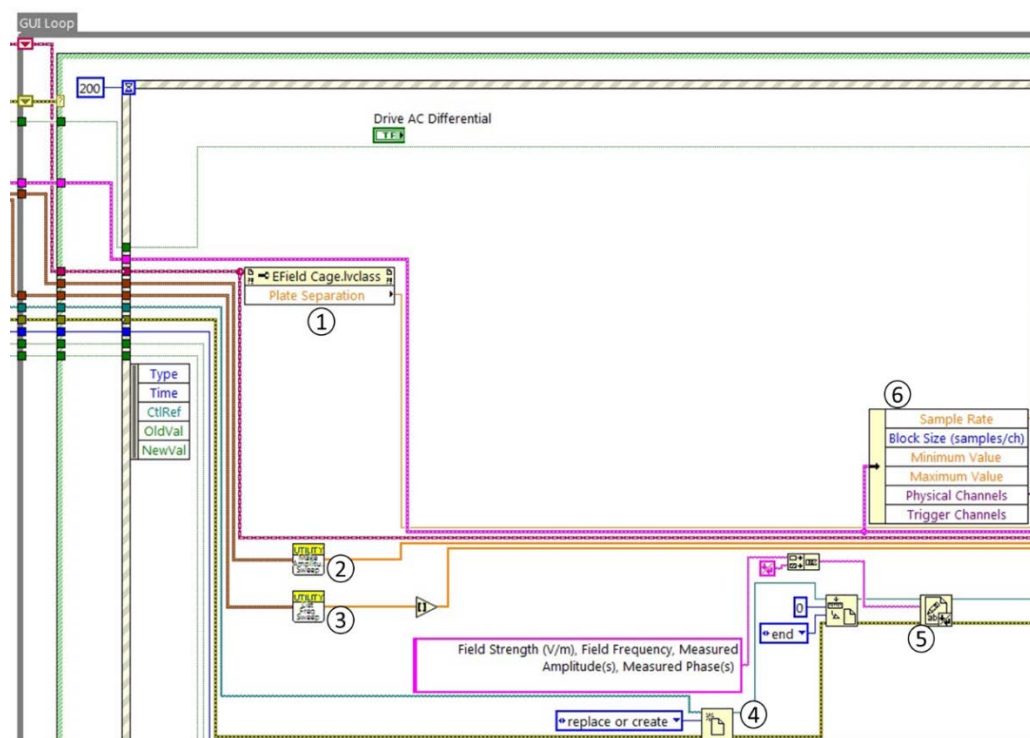As shown in Fig. C-4, arrays (1) must be initialized to store values between iterations of the nested for loops; the outer loop (2) corresponds to each point in the "amplitude sweep settings" array while the inner loop (3) repeats for each point in the "frequency sweep settings" array. A custom VI (5) performs a 1-s fast Fourier transform (FFT) measurement and extracts the sensor output and phase values in the FFT corresponding to the tested frequency, as well as preserving the time-domain waveform captured during the 1-s FFT.
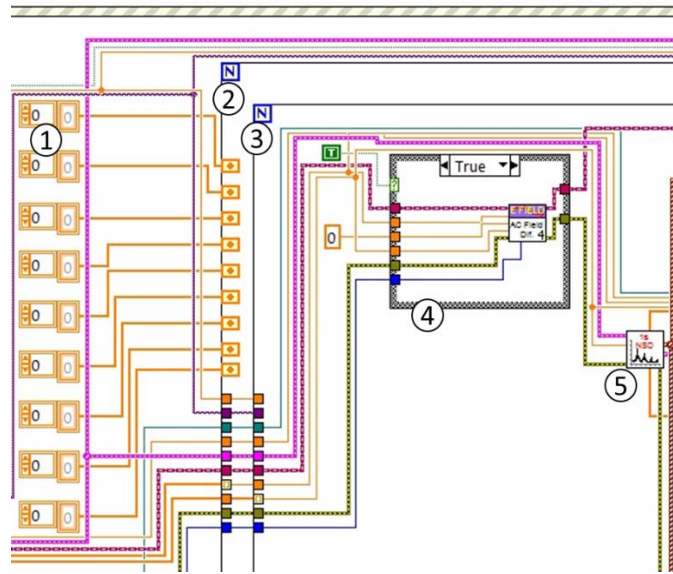

Fig. C-4 Function generator output values established and a 1-s measurement is performed

The current voltage amplitude, frequency, DC offset, plate separation, and cage impedance parameters are then passed into another custom VI (4) to create and set the function generator to appropriate output settings. This VI uses the cage impedance parameter to set the function generator output to either a high or low impedance setting. The amplitude value and plate separation are normalized to a standard electric-field unit of V_{pp} per meter and the V_{pp} value is set on the function generator, which later will be mathematically converted to V_{rms} per meter.

The results from the measurement are plotted in the time domain (1) on the front panel of Fig. C-5. The extracted phase value of every sensor output is combined into an array and the trigger-channel waveform phase is used to convert into a relative phase for each sensor output (2) and (3). The measured sensor output is multiplied by the calibration constant (5) to create the calibrated sensor response described earlier.
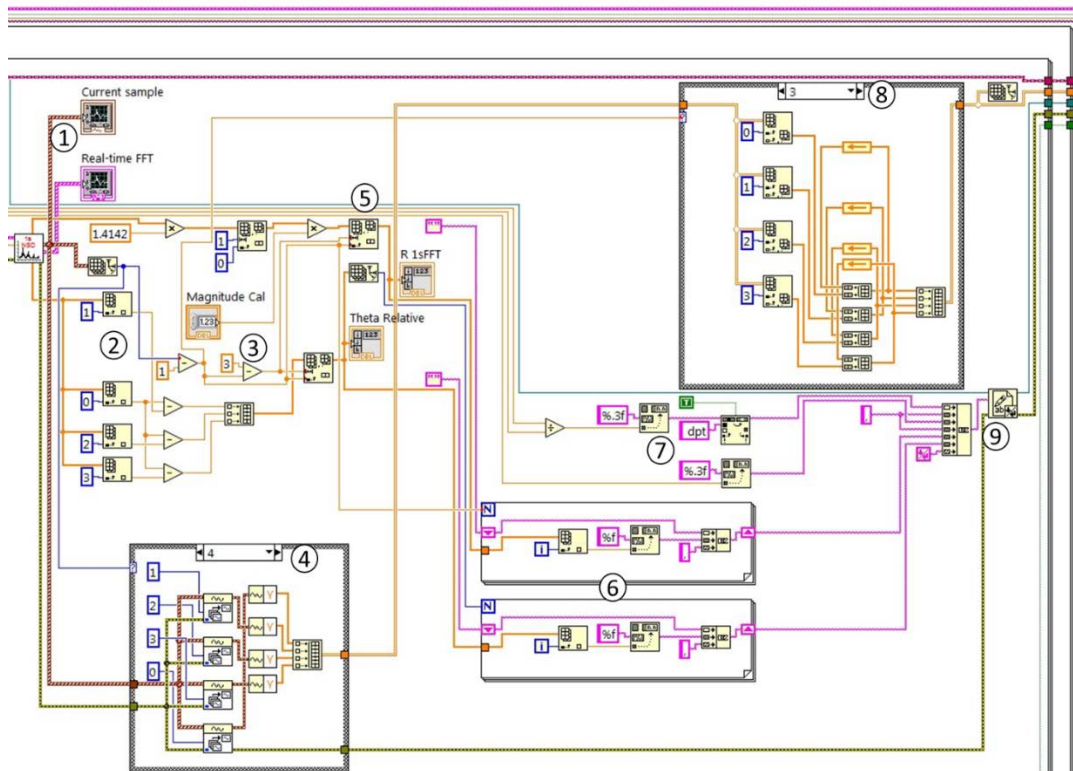
Fig. C-5 Postmeasurement processing and data capture of the frequency response

The time-domain trigger signal and sensor output are converted into arrays (4) and stored between passes of the M×N test matrix (8), which will be stored into an Excel file if the "Log Raw Data" Boolean of the front panel is set to true. The relative phases and test frequency are converted into strings (6), as well as the calibrated sensor magnitude (7). The strings from (6) and (7) are organized and inserted into an Excel file, which by the final loop pass will contain all electric-field magnitudes, electric-field frequencies, calibrated sensor magnitudes, and relative phase measurements made during the M×N test matrix.

C-3 Total Harmonic Distortion (THD)

The function generator (Fig. C-6) is set to a sinusoidal 93-Hz signal for the total harmonic distortion (THD) measurement (1). The ADC measurement units (2), sample rate (3), and sample length (4) are set for a 1-s measurement. An FFT of the measurement is taken (5) and plotted (6) on the front panel.

Fig. C-6 Performing 1-s THD measurement

The sensor output to the first 5 tone harmonics are extracted from the sensor output FFT (1) then used for calculation (3) (4) of an estimated sensor THD value (5). An Excel file is created (2) to store the FFT data after conversion to a string (6), which is used to create more versatile graphs in Excel or MATLAB software.

Fig. C-7 Post-measurement processing and data capture of the THD

C-4 Noise Spectral Density (NSD)

The electric-cage endplates are grounded and a 1-s measurement is taken (1), as shown in Fig. 8. The user is then prompted to short-circuit the sensor frontend

transducer and hit OK (2), then a second measurement is taken. The user is finally asked to disconnect the sensor and ground all ADC inputs (3), for a final 1-s FFT to measure the noise of the hardware. The data from the 3 nose measurements are converted into strings and stored in 3 different Excel files (4) (5) (6), which are then saved and closed (7) (8) (9) to end the test sequence.
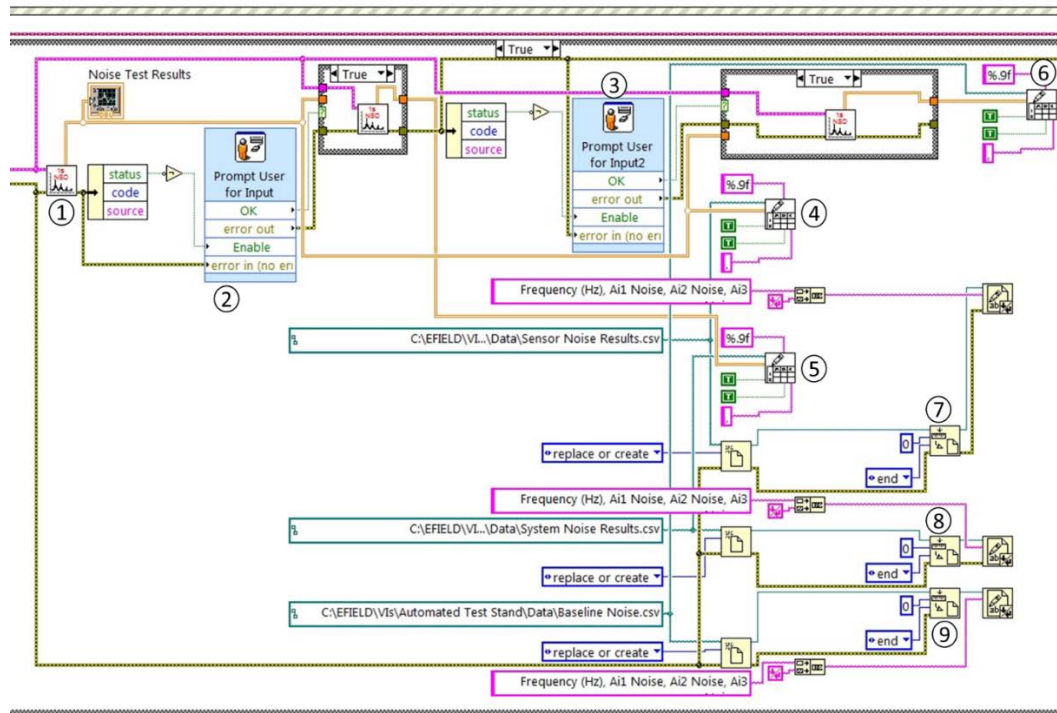

Fig. C-8 NSD measurement performed by LabVIEW code

INTENTIONALLY LEFT BLANK.

List of Symbols, Abbreviations, and Acronyms

AC   alternating current

ADC   analog-to-digital converter

ARL   US Army Research Laboratory

BNC   Bayonet Neill–Concelman

DC   direct current

EFNSD   electric-field-referred noise spectral density

FFT   fast Fourier transform

GRS   ground reference sensor

IEEE   Institute of Electrical and Electronics Engineers

MoM   method of moments

NSD   noise spectral density

PLL   phase-locked loop

PXIe   Peripheral Component Interconnect Extensions for Instrumentation

Std   Standard

THD   total harmonic distortion

TTL   transistor–transistor logic

USB   universal serial bus

VI   virtual instrument

1   DEFENSE TECH INFO CTR
(PDF)   DTIC OCA

         2   US ARMY RSRCH LAB
(PDF)   IMAL HRA MAIL & RECORDS MGMT
               RDRL CIO L TECHL LIB

         1   GOVT PRNTG OFC
(PDF)   A MALHOTRA

         1   US ARMY RSRCH LAB
(PDF)   RDRL-SES P S HEINTZELMAN